

IAC-06-C4.4.7

THE INNOVATIVE DUAL-STAGE 4-GRID ION THRUSTER CONCEPT – THEORY AND EXPERIMENTAL RESULTS

Cristina Bramanti, Roger Walker,
ESA-ESTEC, Keplerlaan 1, 2201 AZ Noordwijk, The Netherlands
Cristina.Bramanti@esa.int, Roger.Walker@esa.int

Orson Sutherland, Rod Boswell, Christine Charles
*Plasma Research Laboratory, Research School of Physical Sciences and Engineering,
The Australian National University, Canberra, ACT 0200, Australia*
orson.sutherland@anu.edu.au, rod.boswell@anu.edu.au, christine.charles@anu.edu.au

David Fearn
EP Solutions, 23 Bowenhurst Road, Church Crookham, Fleet, Hants, GU52 6HS, United Kingdom
dg.fearn@virgin.net

Jose Gonzalez Del Amo, Marika Orlandi
ESA-ESTEC, Keplerlaan 1, 2201 AZ Noordwijk, The Netherlands
Jose.Gonzalez@esa.int, Marika.Orlandi@esa.int

ABSTRACT

A new concept for an advanced “Dual-Stage 4-Grid” (DS4G) ion thruster has been proposed which draws inspiration from Controlled Thermonuclear Reactor (CTR) experiments. The DS4G concept is able to operate at very high specific impulse, power and thrust density values well in excess of conventional 3-grid ion thrusters at the expense of a higher power-to-thrust ratio. A small low-power experimental laboratory model was designed and built under a preliminary research, development and test programme, and its performance was measured during an extensive test campaign, which proved the practical feasibility of the overall concept and demonstrated the performance predicted by analytical and simulation models. In the present paper, the basic concept of the DS4G ion thruster is presented, along with the design, operating parameters and measured performance obtained from the first and second phases of the experimental campaign. Finally, the implications of these findings for future gridded ion thruster developments and future mission applications are addressed.

INTRODUCTION

For over 20 years, ion sources, coupled with charge-exchange gas cells, have been used to inject highly energetic neutral particles (80-100 keV) into fusion reactor experiments²⁻⁵. These ion sources are remarkably similar in design to gridded ion thrusters (without external neutraliser) with the exception that they use 4-grid systems in order to achieve extremely high accelerating potentials and hence ion velocities with light gases such as hydrogen. This 4-grid configuration allows the ion extraction and ion acceleration processes to be decoupled, essentially creating a dual-stage system. The CTR dual-stage ion sources were only 10-40cm in beam diameter, but managed to process input powers from 250kW to 4.8MW and accelerated ionised hydrogen to exhaust

velocities of up to 4,000 km/s. One of the maximum cases recorded experimentally was at the Culham Laboratory, Oxford, UK with neutral atomic beam injectors developed for the JET tokamak². Extremely high power densities of 6670 W/cm² were achieved.

A new thruster concept, the Dual-Stage 4-Grid (DS4G) ion thruster, has been proposed by D. Fearn¹ and drew inspiration from the above mentioned Controlled Thermonuclear Reactor (CTR) experiments.

Due to the high beam potential, the Dual-Stage 4-Grid ion thruster concept is theoretically able to deliver substantial improvements in propulsive performance over the current state-of-the-art gridded ion engines in terms of specific impulse, power and thrust density, maximum power and beam divergence at the cost of a higher specific power. For example, a single 20 cm diameter 4-grid ion thruster could operate at 250 kW power to produce a 2.5 N thrust and a specific impulse of 19,300 s using Xenon

propellant operating at a 30 kV beam potential. These high power and thrust densities allow the maximum attainable power for gridded ion engines to be extended from 40 kW of the present day, to hundreds of kW. This aspect, in combination with the very high specific impulse and a lightweight power system, makes them especially suitable for large, high delta-V future exploration missions, such as 'delivery and return' cargo transportation of surface modules in low orbits of the Moon and Mars needed for human exploration, or even for an advanced human Mars mission itself.

The Advanced Concepts Team of ESA, after having envisaged the potential and assessed possible applications of this concept, awarded a contract to Australian National University for the design and construction of a small experimental laboratory model thruster to be tested at the ESA-ESTEC Propulsion Laboratory.

This paper is aimed at the presentation of the results of the proof-of-concept experimental research project on the Dual-Stage Four Grids (DS4G) ion thruster. The experimental test campaign comprised two successful test phases which were conducted in the CORONA vacuum facility at ESTEC during November 2005 and May 2006, with the aim of demonstrating the practical feasibility of the 4-grids concept, verifying the high performance predicted by the analytical and simulation models, and investigating critical design issues and technological challenges.

In the following sections, the basic concept of the DS4G ion thruster will be presented; in particular, the design, operating parameters as well as the performance obtained from the experimental test campaigns. The measurements performed by the diagnostics tools will then be illustrated. Finally, the implications of these findings for future gridded ion thruster developments and future missions will be addressed.

DUAL-STAGE 4-GRID (DS4G) CONCEPT

Electrostatic grid systems used in conventional state-of-the-art ion thrusters perform ion extraction & acceleration simultaneously in a single-stage process, typically using three permeable grids closely spaced in series. In this scheme, the thruster body and screen grid are at a high enough beam accelerating potential necessary to achieve the ion beam velocity required. To raise the ion velocity, and thus the specific impulse, it is merely necessary to increase the beam potential as appropriate. This ultimately limits achievable performance in terms of power density, thrust density, exhaust velocity, and specific impulse because the inter-grid accelerating potential must be

limited in order to avoid excessive penetration of the grid electric field into the discharge chamber containing the plasma. The resulting effect of this penetration is a curvature in the plasma sheath (or meniscus) attached to the holes in the screen (first) grid. Some penetration is desirable, since these results in a curved plasma sheath which both increases the ion emission area and aids focusing. Unfortunately, the higher the beam potential, the greater the curvature, and hence the greater the extracted ion beamlet divergence, until significant direct ion impingement occurs on the acceleration (second) grid and deceleration (third) grid.

Direct impingement of energetic ions causes sputtering of the grid material, leading to excessive grid erosion (essentially hole widening), performance degradation and eventually limitation of thruster lifetime. Moreover, the plasma number density, n , in the discharge chamber must also be taken into account, since the penetration of the sheath increases as n falls. This problem is relevant to the use of a wide throttling range⁶, or if the radial plasma density distribution is strongly peaked. However, in the latter case the dimensions of the screen grid apertures can be matched to this distribution to alleviate adverse effects⁷. Thus it is clear that high values of E and/or low values of n allow the sheath to penetrate deeply into the plasma. The resulting curvature of the surface from which the ions are extracted causes many of the trajectories to diverge from the desired paraxial direction, and to impact upon the accel or decel grids. The erosion that this causes severely limits lifetime⁸.

This situation is depicted in Fig 1, in which the

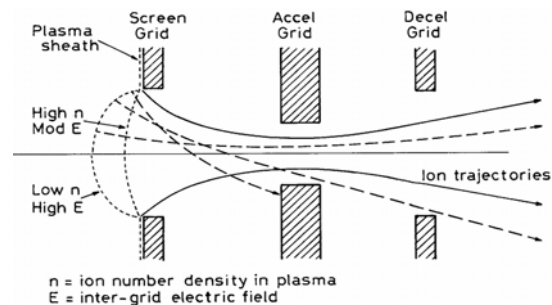


Figure 1. Triple grid configuration, indicating the effects of the sheath shape on ion trajectories sheath positions for a moderate and a high electric field, E , are shown.

In order to avoid beamlet divergence, impingement and sputtering, grid accelerating potential is limited to a maximum of about 5 kV in present systems (usually much less). Practically, this limits the achievable specific impulse to $<10,000$ s, thrust density to <0.5 mN/cm², and power density to <20 W/cm² with Xenon propellant. Due to these performance limits and

thermal/mechanical constraints placed on the thin, closely spaced grids, present gridded ion thrusters operate at powers of up to 40-50 kW maximum with beam apertures of up to order 50 cm diameter.

This problem is avoided by the use of 4 grids, since the extraction field is defined by the first two of these (Fig 2). As previously mentioned, this configuration was originated in the controlled thermonuclear reaction (CTR) research community in order to produce very high energy particles for injection into fusion machines. Plasma sources fitted with such grid systems are used to accelerate ions, usually hydrogen, to energies that can reach MeV. They are then passed through a charge-exchange gas cell to produce the required high energy beams of neutral atoms. These are necessary to penetrate the large magnetic fields within fusion devices.

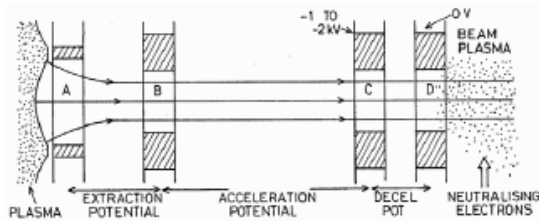


Figure 2. Schematic diagram of the 4-grids system.

The 4-grid system allows the ion extraction and ion acceleration processes to be decoupled, essentially creating a dual-stage system instead of the usual three grid thrusters where the two processes must occur simultaneously, leading to a practical limitation in the maximum beam potential to <5 kV. In the first stage of the 4-grid concept, ions are extracted from the discharge chamber using the first two grids with the potential limited to <5kV to prevent excessive plasma sheath curvature and hence direct impingement of the extracted ions on the grids. Then, in a longer second stage between the two pairs of grids, they are accelerated to much higher velocities with acceleration potentials of up to 80 kV.

The bulk of the acceleration then occurs between the second and third grids, which can be widely separated to accommodate the potential applied, which can be very large. The negative third grid acts in the same way as the accel grid in the conventional two or three electrode system. An important function is to repel the electrons in the external plasma, thereby preventing electron “backstreaming”. The 4th grid behaves as the decel grid in the triple-grid scheme, reducing the total aggregate sputtering damage due to charge-exchange ions. It can be at zero (space) potential or slightly negative.

A further potential benefit of the dual-stage system is a very low beam divergence of about 2-6 deg only due to the strong acceleration of the second stage, thus reducing further any possibility of adverse thruster-spacecraft interactions, and also attitude control demands when compared to other thrusters. Present gridded ion thrusters have typical divergence of 12-15 deg, and Hall effect thrusters about 40 deg. Fig 3 shows a schematic of the 4-grid ion thruster concept.

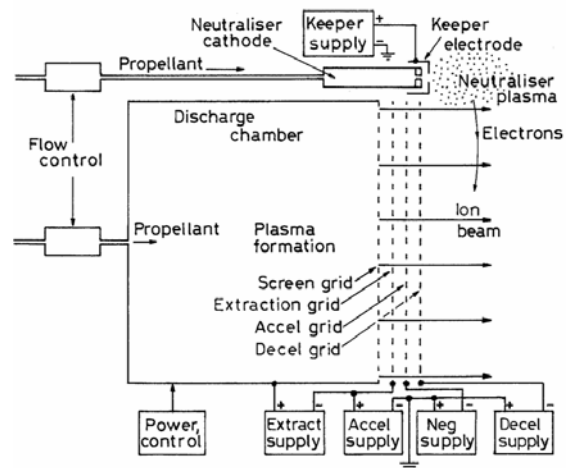


Figure 3. Schematic diagram of a 4-grid ion thruster.

LABORATORY PROTOTYPE DESIGN

The initial proof-of-concept programme, initiated in June 2005, involved the development and testing of a small low-power laboratory model prototype thruster, which was designed and built by the Space Plasma and Plasma Processing Group at the Australian National University (ANU) based on advances that were made at the ANU on RF plasma sources, the RF feeds, and high voltage electrodes under previous research activities not relating to this project.

The original plan of the programme was to test a Single Aperture Four Electrode (SAFE) configuration with a single 1 mm diameter aperture only, but this changed to also consider a 4-grid system consisting of 43 apertures of 1 mm diameter in order to fully demonstrate the DS4G concept. Most of the beam tests were performed on the latter at higher thrust, once high voltage beams were shown to be extracted reliably from the SAFE configuration without direct ion impingement.

The laboratory prototype thruster is shown in a sectional view in Figure 4, with the gas inlet at the top and the grid assembly at the bottom.

A photograph is presented in Figure 5, in which the edges of the grids can be seen at bottom right. The

thruster was based on a 5 cm diameter cylindrical discharge chamber made from ceramic and fed with a regulated flow of Xenon gas.

The Radio-Frequency (RF) discharge was energised by a 3-turn antenna coiled around the discharge chamber, biased to the screen grid voltage; this is not shown in the figures. This antenna was fed from a manually-tuned RF system operating at 13.56 MHz. A high voltage 4-grid system, connected to appropriate power supplies, was attached to the discharge chamber in order to extract ions from the plasma and accelerate them electrostatically via the two-stage process discussed above. Under suitable conditions, this resulted in the desired highly focussed energetic ion beam.

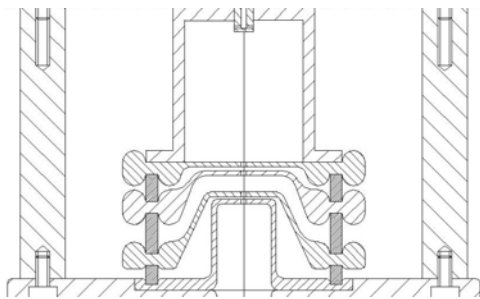


Figure 4. Schematic of the thruster

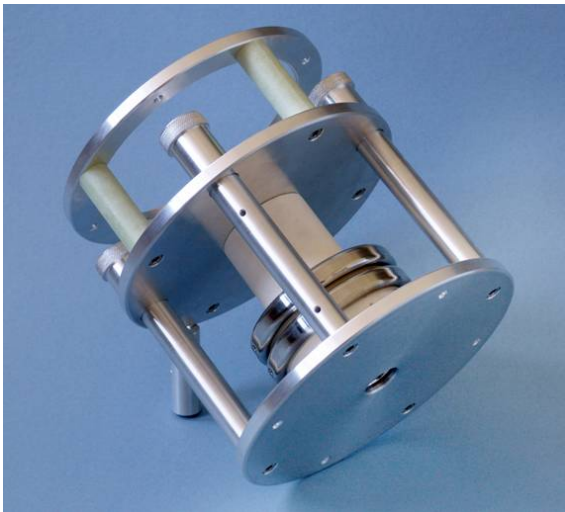


Figure 5. Photograph of the thruster

The lab model tested here is not suitable or applicable for space use, it is only intended to demonstrate the principle at low-cost, test viable ion optics and identify any critical issues for the future. It consists of three subsystems namely:

- Mechanical subsystem: clamping mechanism including aluminium clamp end plates, clamp posts, and thrust balance mounting ring

- Radio-Frequency (RF) subsystem: gas injector, ceramic plasma source tube, 3-turn antenna, stand-off transformer, impedance matching box, RF generator
- High Voltage (HV) subsystem: interchangeable grid module with four grids and three ceramic inter-grid spacer rings, HV vacuum feedthroughs & connectors, two HV power supplies rated to maximum voltage of 35 kV and current of 80 mA and one LV power supply.

EXPERIMENTAL TEST DESCRIPTION

Two separate tests were performed in the CORONA vacuum facility at ESTEC during November 2005 and May 2006. The main chamber of CORONA is 2 m in diameter and 4 m in length and it contains the computer-controlled beam diagnostic equipment on motorised arms for ion beam scanning with mounted diagnostic probes sweeping over wide angles. CORONA also has a 1 x 1 m secondary hatch vacuum chamber which contains a thrust balance or thruster mounting rig and the thruster. This can be isolated from the main chamber via a gate valve to allow quick thruster modifications without the need to vent the main chamber. Vacuum levels down to 10^{-8} millibars are reached.

The DS4G thruster was mounted on the thrust balance inside the CORONA secondary hatch chamber, the gate valve between the hatch and the main chamber could be opened to allow the thruster ion beam to travel 4 m into a large volume before colliding with the graphite target. No active neutralizer was used in the experiments, hence any neutralization of the beam would be by secondary electron emission from the target. Diagnostic equipment mounted on arms took measurements of the ion beam at a distance of 1.5 m from the thruster exit plane. The setup of the thruster inside the hatch is shown in Fig 6. The principal aims of the first experimental test were to:

- Demonstrate the theoretical performance (very high expected specific impulse, power and thrust densities) of a dual-stage 4-grid ion extraction/acceleration system operating at beam potential up to 30 kV with Xenon propellant for future application to spacecraft gridded ion thrusters
- Characterise the extracted ion beam (very low expected divergence) and performance over variations in plasma density, extraction potential and beam potentials

- Attempt to optimise ion optics for grid lifetime (minimise grid impingement currents by varying extraction potential).

During this phase, a series of beam test firings were performed with the DS4G laboratory prototype thruster under high vacuum conditions. During each beam test, data was acquired on the thruster operating parameters, grid currents and voltages, and beam characteristics through the use of dedicated beam diagnostic tools, including:

- Single-electrode Langmuir probe (electron temperature and plasma potential of the plasma surrounding the beam)
- Faraday cup (current density in the beam)
- Electrostatic wires (beam divergence calculated from 95% of the collected current on the voltage-biased wires integrated over angle from thruster bore axis)

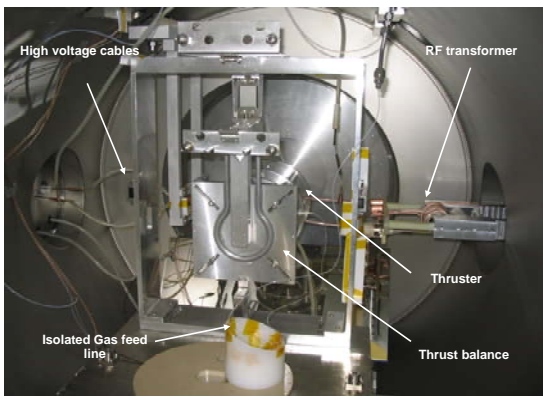


Figure 6. Test configuration of the DS4G laboratory prototype thruster mounted on a thrust balance inside the CORONA hatch

From analyzing the results obtained from the first test phase, it was apparent that the efficiency of the

laboratory prototype thruster was very low compared to conventional ion thrusters (no requirement was originally set for this parameter).

In order to make an attempt to obtain an improvement in this area, it was decided to revise the grid ion optics design and so a second test was carried out with new grids incorporating the revised optics specified by ESA. The main objectives of the second experimental test were to:

- Experimentally validate the new grid ion optics design in order to improve the efficiency of the thruster similar to or greater than that of conventional ion thrusters
- Characterise the plasma density in the source tube as a function of the RF power and the mass flow rate in order to improve the knowledge of conditions close to the plasma sheath
- Characterise and refine the performance of the thruster with the new grid sets at different operating points (beam current and beam potential) with Xenon propellant
- Characterise the ion beam optics (grid impingement, divergence) and extracted beam (current density, beam plasma parameters) for each of the test configurations and operating points.

During this second phase, several beam test firings were performed and the thruster control parameters and grid current data were acquired. In addition, new beam diagnostic tools (Fig. 7 and Fig. 8) were developed in-house at ESTEC in order to provide more accurate beam measurements during the test:

- Carbon-shielded Langmuir probe inserted in the high energy ion beam (electron temperature and plasma potential inside the beam) (Fig. 7)
- Carbon front-faced Faraday Cup scanned through the ion beam (beam current and current density, beam divergence calculated from 95% of the collected current distributed over scanning angle from the bore axis) (Fig. 8)
- Carbon front-faced Calorimeter inserted in the high energy ion beam (beam power) (Fig. 7)

In addition, five thin single-electrode

Langmuir probes were inserted through the first grid into the plasma source tube in order to estimate the electron temperature and plasma potential of the plasma inside the source tube. A picture of the experiment is shown in Figure 9.

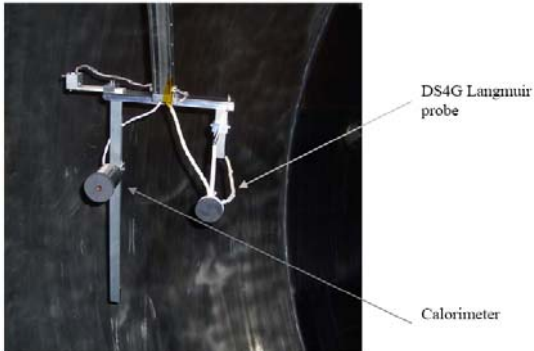


Figure 7. Calorimeter and Langmuir probe mounted in CORONA test facility.

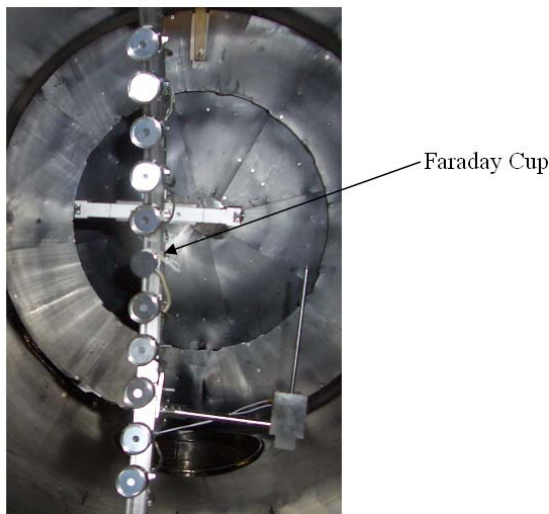


Figure 8: Carbon shielded Faraday cup in the beam mounted with the other non-shielded Faraday cups in the vacuum test facility

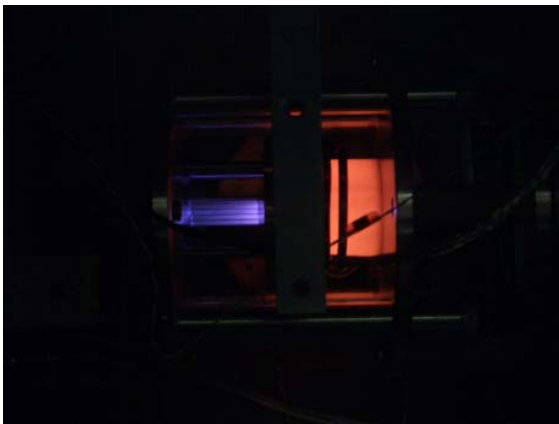


Figure 9. Experimental test with five thin single-electrode Langmuir probes inserted in the discharge chamber

EXPERIMENTAL TEST RESULTS

First phase experimental results

Prior to attempting beam extraction from the DS4G laboratory prototype thruster, thermal and high voltage breakdown tests were performed. The thruster was able to operate with RF plasma discharge at power levels of up to 600 W for over 45 minutes, significantly beyond those expected for the 10-15 minute beam tests, thus giving good margins and confidence in the RF subsystem operation (see Figure 10). Breakdown tests were run with voltages on the first two grids reaching 30 kV and 27 kV respectively in vacuum conditions, providing confidence in the HV subsystem operation.



Figure 10. DS4G laboratory prototype thruster pictures with Xenon RF discharge at 400 W power during thermal testing (no high voltage feedthroughs present)

A summary of the results obtained from the first test is presented in next Table. The values for the typical test case shown are for a beam potential of 25 kV.

Performance parameters	Typical test case	Best value	Operating parameters	Range
Thrust (mN)	2	2.85	Beam potential (kV)	10 - 30
Specific impulse (s)	14,000	15,000	Extraction potential (kV)	3 - 6 (3 optimum)
Total efficiency	0.34	0.34	Beam current (mA)	4 - 12
Mass utilisation efficiency	0.73	0.75	Beam power (W)	100 - 260
Electrical efficiency	0.47	0.47	RF power (W)	100 - 490
Beam divergence (deg)	-	2.5	RF plasma density (cm ⁻³)	2.5 x 10 ¹¹ - 1.23 x 10 ¹²
Grid impingement (%)	2	1	Mass flow rate mg/s (Xe)	0.004 - 0.014
Open Area Thrust density (mN/cm ²)	5.9	8.4	Beam diameter (cm)	2.3
Open Area Beam Power density (W/cm ²)	555	740	Grid open area ratio (%)	8.1
Total Thrust density (mN/cm ²)	0.5	0.7	Beam plasma electron temp (eV)	5.7 - 11.0 (±0.5)
Total Beam Power density (W/cm ²)	45	60	Beam plasma potential (V)	24 - 52 (±2)

Table 1. Summary of DS4G lab prototype performance during the first phase of the experimental campaign tests at ESTEC performed in November 2005.

The test programme was a remarkable success and the dual-stage 4-grid concept was proven to work in practice, in the context of space propulsion, for the first time. The thruster could be operated at beam potentials of up to 30 kV and produced an excellent performance in terms of specific impulse, thrust density and power density (grid open area only), and beam divergence. The values achieved represent an improvement by several times on the current state-of-the-art, whilst maintaining negligible direct ion impingement of the beam on the grids (about 1% was recorded).

Since the thruster was originally designed with one objective in mind, namely to prove the feasibility of the operation of the 4-grid concept at high beam potentials via the use of a single aperture only configuration (this was later changed to the 43-aperture configuration presented in this paper), the grid ion optics were not optimised and the open area ratio was very low, leading to a low extraction area and hence extracted beam power compared to the RF power input. Therefore, the electrical efficiency and hence total efficiency achieved by the thruster were low, even when the propellant utilisation efficiency was relatively high at over 70%.

Second phase experimental results

The need to improve efficiency to typical gridded ion thruster levels before a flight engineering model suitable for spacecraft applications could be

contemplated led to the initiation of a second test utilising a completely revised grid optics design with a considerably increased open area ratio of 61%. This design was based on well-established ion thruster grid system principles, modified as necessary to accommodate the 4th grid.

Prior to the start of the test in May 2006, simulations of the new design verified the new ion optics approach and predicted that much higher beam currents could be achieved for the same RF power due to a grid extraction area over 5 times larger, or conversely a much lower RF power for the same beam power. Table 2 presents the operating parameters of the second test phase and one set of the relevant results obtained during a typical experimental test run and the best values achieved. Further data processing, analysis and interpretation efforts are still ongoing.

Due to the introduction of new ion optics, higher values of electrical efficiency, total efficiency as well as total thrust and power density were reached. The mass utilisation efficiency has been improved from 70% to between 80-96% by specific targeting of the beam current in relation to the mass flow rate (85-92% is typically achieved in conventional RF ion thrusters such as the RIT⁹).

This improvement has also contributed to an increase in the total efficiency to 70% in some cases, similar to that achieved in conventional gridded ion thrusters.

	Typical test case	Best value	Operating parameters	
Thrust (mN)	2.7	5.4	Beam potential (kV)	10 – 17.5
Beam potential (kV)	15	17.5	Extraction potential (kV)	1.5 - 5
Specific impulse (sec)	14000	14500	First electrode (beam) current (mA)	4 -33
Mass utilisation efficiency	0.96	0.96	RF power (W)	20 – 316
Electrical efficiency	0.66	0.75	Beam power (W)	80-398
Total efficiency	0.63	0.7	Total efficiency	0.4-0.7
Beam divergence (deg)	4.6-5.3	3.8	Electrical efficiency	0.5-0.75
Total power (W)	300	614	Beam divergence	3.8-6.2
RF power (W)	101	316	Mass flow rate (mg/sec)	0.01 - 0.05 (Xe)
Thrust density (total) mN/cm ²	0.86	1.7	Beam diameter (cm)	2
Total beam power density (total) W/cm ²	64	126	Grid open area ratio	61 %

Table 2. DS4G lab prototype performance during the second phase of the experimental campaign tests at ESTEC performed in May 2006.

It should be pointed out that these experimental data presented in Table 2 are pessimistic, because they assume that all currents collected by the extraction and accelerator grids are due to direct ion impingement. As a consequence, these grid currents have been subtracted in full from the beam current, as deduced from the electron current to the screen grid, to give a reduced beam current. This has been utilised in calculating thruster performance parameters.

In reality, it is not possible with the available data to assess what the actual impingement currents were, because the current flow to each grid was a combination of particle fluxes from a variety of sources. These were the charge-exchange ions formed within the grid system, secondary electrons produced by ion impact, particles collected from the external plasma, and the direct ion impingement itself. Thus values that might be derived ignoring the currents to the extraction and accelerator grids would be optimistic, and would represent the maximum possible performance in the absence of direct impingement.

This additional assessment was made and, as predicted, the derived performance increases significantly, to typically 3.7 mN at the nominal 2.7 mN thrust level, and to 6.75 mN at 5.4 mN.

It should also be pointed out that there is some uncertainty regarding the values of propellant utilisation efficiency derived from the mass flow rate data. This is because, owing to lack of time, it was not possible to allow the thruster to fully stabilise after altering operating conditions before taking data. So, although the flow controller was certainly giving the correct flow rate, the pressure distribution within the feed system and the thruster had not reached complete equilibrium. It has anyway to be highlighted that a typical test run lasted for about 10 to 15 minutes. To assess accurately the degree of uncertainty resulting

from this departure from steady-state is not simple, since it includes, for example, the way in which the ionisation processes within the discharge chamber respond to pressure changes, but a preliminary assessment suggests that 5% may be a realistic figure.

Figure 11 shows the high energy ion beam produced by the thruster (emanating from the right hand side of the picture) and beam characteristics being measured by the dedicated intrusive diagnostics which can be seen on the left.



Figure 11. The DS4G beam inside the vacuum chamber and the dedicated diagnostics

Some more detailed experimental results are presented below in Figures 12 to 14. As an example of the experimental procedure adopted, Figure 12 shows the increases of RF power and of flow rate applied during Test 56, when the screen grid was at 15 kV and the extraction potential was 5 kV. The resulting increase in beam current, assumed here to equal the

screen grid current, is shown in Figure 13. When corrected for the currents to the extraction and accelerator grids, the thrust generated behaved as indicated in Figure 14. It reached beyond 5 mN.

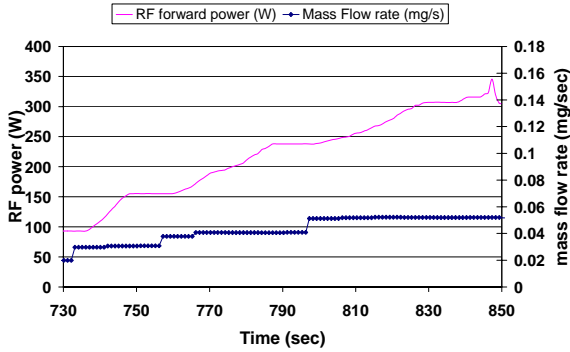


Figure 12. Evolution of the RF input power and the mass flow rate as function of the time test#56

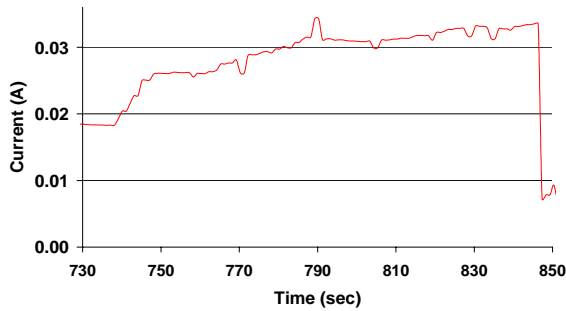


Figure 13. Behavior of the first electrode beam current as function of the time test #56

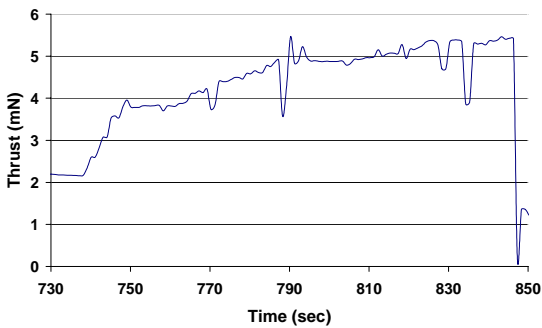


Figure 14. Behavior of the thrust as function of the time test #56

As discussed previously, in evaluating thruster performance the most optimistic results are obtained if it is assumed that there is no direct ion impingement on any of the electrodes. Of course, a practical long-life thruster needs to approximate to this ideal case, so it is relevant to examine how much performance increase might be achieved. This is illustrated in Figure 15, in which the currents to the extraction and

accelerator grids have not been subtracted from the screen grid current. It is clear that the performance increase is considerable, reaching a thrust level well in excess of 6 mN.

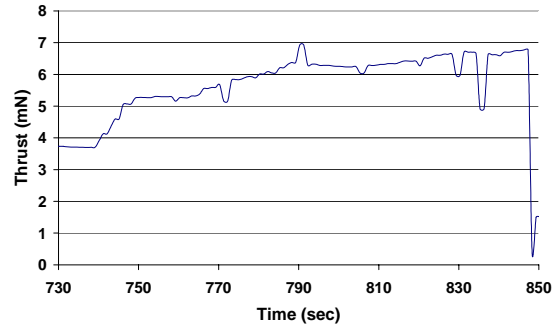


Figure 15. Behavior of the thrust as a function of time in Test #56. The currents to the 2nd and 3rd electrodes have not been deducted from the screen grid current.

The effect of extraction potential on screen grid current, and thus on beam current, is illustrated in Figure 16 for two values of RF power and constant flow rate. As expected, the current increased quite rapidly with potential, and thus with grid perveance, confirming that the plasma number density in the discharge chamber plasma was fully sufficient to provide the necessary ion flux under this range of conditions. Thus, assuming that the ion optics were able to operate successfully over this range, extensive throttling would be entirely feasible.

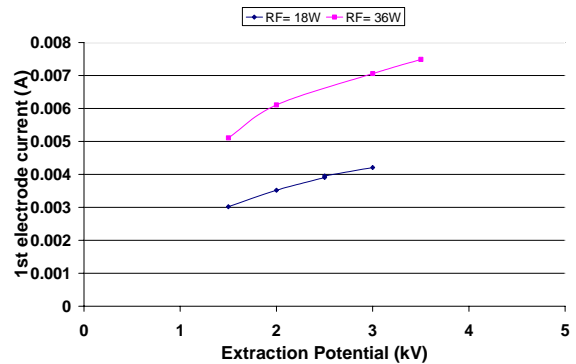


Figure 16. Behavior of the first electrode beam current as function of the extraction potential for two RF input power. (mass flow rate = 0.015 mg/sec, first electrode voltage = 10kV).

The ion beam profile was measured at a distance of 1.5 m from the thruster using a Faraday cup probe designed specifically for this high beam energy application. Typical results are shown in Figures 17 and 18, in which actual beam current within each radial position is plotted against radius. Bearing in

mind the very low current density at this distance from the thruster and the electrical noise present, these curves are very smooth and symmetrical, and can be regarded as fully satisfactory.

The beam divergence was derived from these plots; it was defined as the beam half-angle containing 95% of the total beam current. As can be seen, the values of divergence were very low, at just over 5°, which is far better than ever recorded with a conventional ion thruster.

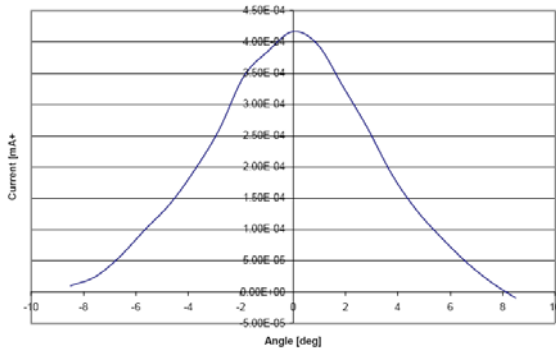


Figure 17. Beam profile test #45 (mass flow rate=0.02 mg/sec, RF power=60W, V1=17.5kV V2=12.5 KV). Derived divergence =5.4 deg.

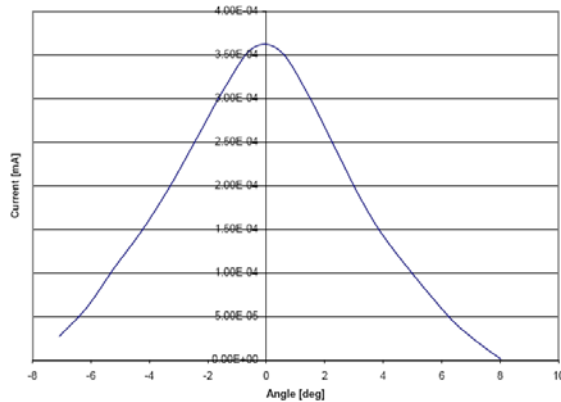


Figure 18. Beam profile from Test #43 (mass flow rate = 0.02 mg/sec, RF power = 150W, V1 = 15 kV V2 = 10 kV). Derived divergence = 5.2 deg.

The beam power density has been derived from the measurements performed by the calorimeter, which was positioned 1.5m far from the thruster exit and in the center. The following Figure shows the temperature profile as function of time recorded by the calorimeter for the Test 53. The derived beam power density was 0.06 W/cm². In order to verify the validity of the measurement, the above result has been compared with the beam power density peach measured by Faraday cup in the same test (screen grid voltage 15kV and first electrode beam current 20mA), which resulted about 0.04 W/cm². Those results

provide a high confidence level on the effective design of the diagnostic tools.

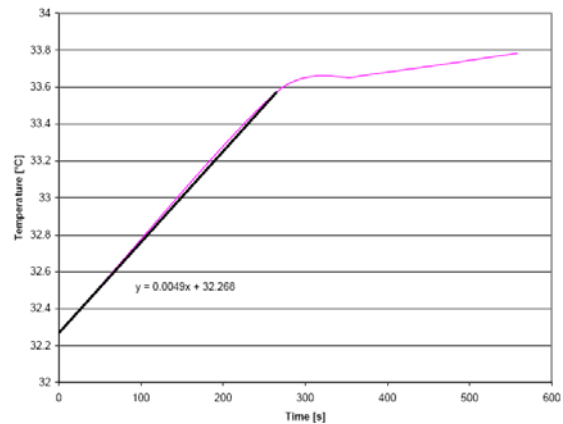


Figure 19. Temperature profile test #53 (First electrode current =20mA, V1=15kV V2=10 KV).

CRITICAL ENGINEERING CHALLENGES

As a consequence of operating a gridded ion thruster at significantly higher power and thrust densities and exhaust velocities, enabled by the high voltage dual-stage 4-grid system, a number of engineering issues will need to be addressed. These are discussed below.

The higher discharge power needed to supply an increased plasma density in the discharge chamber will lead to a high chamber external temperature. Whilst this is unlikely to cause mechanical breakdown of discharge chamber structure/materials, thermal aspects need to be assessed and an adequate thermal control system incorporated as necessary. Solenoid windings, harness, and grids are particularly sensitive and may need to be thermally isolated from the chamber.

In order to prevent high voltage breakdown phenomena occurring which could severely disrupt thruster operations, attention should be paid to the design of the high voltage grid system, in addition to reducing charge-exchange ions in the inter-grid gaps and the effective isolation of the gas feed system from the discharge chamber. If this is not possible, solutions involving a floated propellant storage and distribution system should be investigated.

With high grid voltages at 10-30 kV, new Power Processing Units supplying the thrusters with regulated DC-DC conversion from the low-voltage main spacecraft bus would need to be developed and attention paid to the electrical isolation of the high voltage parts of the whole system from the spacecraft. Conventional PPUs tend to have a high specific mass

and thus are not attractive. These units (usually the dominant mass driver in the EP system) can be eliminated through the use of direct drive from a nuclear power source. New high-tension harnesses will need to be space-qualified, and adequate isolation of thruster/harness/connectors from the spacecraft ensured during spacecraft integration.

Due to the high plasma density in the discharge chamber, internal erosion of the discharge chamber materials due to sputtering could be evident over long operation times. The application of sputter-resistant coatings such as tantalum or graphite to the inside of the discharge chamber would alleviate this problem. Alternatively, the discharge chamber could be manufactured from graphite.

By far the most concerning issue for limiting thruster lifetime is grid erosion due to sputtering from ion impingement. The high acceleration potential between extraction and accel/decel grids will ensure a very low beam divergence in the acceleration stage. Beamlet width in the grid holes (perveance) will be dictated by the extraction potential and beam current density. The thruster operation can be de-rated from the maximum perveance by limiting extraction potential (below 5 kV) and beam current density to ensure extracted beamlets are well within their grid holes. Despite this, some ion impingement will occur (including charge exchange ions), so it would be prudent to use grids manufactured from low sputter rate materials such as graphite, as demonstrated on many state-of-the-art conventional 3-grid thrusters.

MISSION APPLICATIONS

The limit on specific impulse of about 10,000 s with Xenon inherent in 3-grid systems does not present a problem for missions to bodies in the inner solar system or those out to Jupiter, since typically their optimum values are lower than this maximum for reasonable mission durations (e.g. 2,000-6,000 s for Mars round trips, 8,000-10,000 s for Jupiter Icy Moon Orbiters) with present day power system technologies. However, it is evident that missions to the far outer solar system and beyond, such as Pluto/Kuiper Belt Object (KBO) Orbiters, inner Oort cloud flyby and 100-250 AU Interstellar Precursor missions, will need specific impulse values beyond 10,000 s in order to ensure that propellant mass fraction does not dominate the spacecraft mass budget for the high delta-V concerned (25-50 km/s). Hence, the 4-grid thruster concept demonstrated successfully in the presented experimental programme is ideally suitable for these classes of missions. The potential pay-offs for very high specific impulse delta-V missions such as these include reduced transfer time, increased scientific and

communications payload mass and very relaxed Earth escape launch window requirements.

Preliminary technology assessment and mission optimisation studies¹⁰⁻¹¹ indicate that significant benefits for local interstellar probe missions to 200 AU for example can be obtained by employing the 4-grid ion thruster concept (this also applies to other extreme outer solar system missions). An optimum design solution was found for an 8000 kg spacecraft wet mass, 400 kg payload, with 65 kW reactor and DS4G-type thruster operating at 10,200 seconds specific impulse and thrust of 0.9 N. A single 25 cm diameter DS4G-type thruster with a beam potential of 13000 Volts would be sufficient for these requirements. The benefits compared to a 1-ton, 1 kW-class RTG-powered 3-grid ion thruster spacecraft include reduced trip time (23 years compared to 30 years), increased payload mass (several hundreds of kg may be available), lower C3 launch energy (16 instead of 140 km²/s² which could be delivered by Ariane 5), and wider launch windows/lower radiation dose (no close Jupiter swingby needed). The disadvantage of this solution is the high development cost associated with the nuclear reactor power system. Due to the high power-to-thrust ratio associated with such a high specific impulse (around 90 kW/N for a specific impulse of 15,000 s), it is clear that an electric propulsion system employing the 4-grid concept is only compatible with lightweight (i.e. low specific mass) power systems. In the case of Nuclear Electric Propulsion (NEP), Radioisotope Thermoelectric Generators (RTGs) have a specific mass (of over 200 kg/kW) which is far too high for the 4-grid thruster. The development of a low specific mass space nuclear reactor (of the order of 25 kg/kW or less) would therefore be required. One possible solution is the use of more advanced high efficiency energy conversion systems such as dynamic Brayton cycle engines that are able to operate reliably for over 10 years. This still needs to be developed and demonstrated both on ground and in space.

The limits on power density and thrust density severely affect the suitability of present gridded ion thrusters to high power robotic and human missions to any destination however. The only method to deliver the N-level thrusts required for larger payload missions with these limitations is to increase the beam aperture area and hence the thruster diameter and mass. Unfortunately, due to thermal and launch vibration constraints, the thin grids have a maximum diameter of about 50 cm. Due to these constraints, present gridded ion thrusters operate at powers from 1-40 kW and thrusts the 10-1000 mN range, and their absolute limit is considered to be 40 kW. This leads to the necessity of using a large module integrating a cluster of thrusters with a number of power processing

units for missions in the 100 kW-MW class, thus leading to a high propulsion system mass and volume. Taken to the extreme, a human Mars mission using EP would require about 8-15 MW power and deliver a thrust of 90-180 N. Using conventional gridded ion thrusters (or indeed Hall effect thrusters) limited to 50 kW power would require some 160-320 thruster units each of 50 cm diameter, thus requiring complex on-orbit assembly. Even using the alternative approach of spacing multiple grid systems over the interface with a single large area discharge chamber to extend thruster power levels to the 100kW range still results in a very large thruster, and does not reduce the mass and volume substantially. For this reason, alternative propulsion technologies able to accept higher power and thrust within a compact device and deliver moderate/high specific impulse are being investigated for the 100 kW-MW mission class. Examples include Magneto-Plasma-Dynamic (MPD) and Helicon RF Plasma thrusters (e.g. VASIMR or HDLT).

The high power and thrust densities (and specific impulses) delivered by the 4-grid thruster as a result of the high beam potential (15-30 kV) make it suitable for very high power, high delta-V missions such as reusable Mars heavy cargo 'delivery and return' tugs with 100-500 kW power levels provided by lightweight thin film solar arrays, interstellar precursor or KBO/Oort cloud object flybys using the same lightweight solar array technology, and advanced human Mars missions of MW power levels provided by a lightweight nuclear reactor. Further work is planned on the application and optimization of the 4-grid thruster to the solar electric propulsion mission/system concepts.

CONCLUSIONS

An experimental programme conducted recently with a small low-power laboratory prototype thruster has demonstrated the viability of the dual-stage 4-grid ion extraction and acceleration concept. Total accelerating potentials of up to 30 kV were demonstrated. Narrow beam divergences of the order of $2-4^\circ$ were also achieved. The SI reached 14,000-15,000 s and the open area thrust and power densities 8.4 mN/cm^2 and 740 W/cm^2 , respectively. Total efficiencies of 70% and thrust over 5mN were obtained due to the introduction of new grid ion optics for high electrical efficiency, and a high propellant utilization efficiency of the RF plasma source used.

The diagnostic tools, which have been designed and developed specifically for characterizing this high energetic beam, have been validated and enabled to characterize the beam power density and beam divergence.

These results are encouraging, and pave the way for future work to further develop the concept. The cost of this high performance is a high power-to-thrust ratio, which implies that the 4-grid concept is only compatible with lightweight nuclear and solar power systems which still need to be developed and demonstrated. However, some advanced missions are enabled with this promising concept once progress in power system technology is made. Therefore, it is concluded that the future benefits justify the research and development effort made.

ACKNOWLEDGEMENTS

The authors would like to acknowledge the technical staff at ANU, Peter Alexander and Dennis Gibson, who built the laboratory prototype thruster. The authors also express their gratitude to Dr. Franco Ongaro, Dr. Giorgio Saccoccia, Dr. Leopold Summerer, Mr. Andrés Gálvez, Dr. Bruno Sarti, Mr. Philippe Meijgaarden and the Workshop team from ESA for their continuous support and encouragement.

REFERENCES

- ¹ Fearn, D G, "The use of ion thrusters for orbit raising", *J Brit Interplan Soc*, **33**, 129-137, (1980).
- ² Martin, A R, "High power beams for neutral injection heating", *Vacuum*, **34**, 1-2, 17-24, (1984).
- ³ Okumura, Y, et al, "Quasi-dc extraction of 70 keV, 5 A ion beam," *Rev Sci Instrum*, **51**, 728-734, (1980).
- ⁴ Menon, M M, et al, "Power transmission characteristics of a two-stage multiaperture neutral beam source," *Rev Sci Instrum*, **51**, 1163-1167, (1980).
- ⁵ Ohara, Y, "Numerical simulation for design of a two-stage acceleration system in a megawatt power ion source," *J Appl Phys*, **49**, 4711-4717, (1978).
- ⁶ Mundy, D H and Fearn, D G, "Throttling the T5 ion engine over a wide thrust range", AIAA Paper 97-3196, (1997).
- ⁷ Bond, R A, Fearn, D G, Wallace, N C and Mundy, D H, "The optimisation of the UK-10 ion thruster extraction grid system", IEPC Paper 97-138, (1997).
- ⁸ Martin, A R, Banks, C R, Baton, R W, Hurford, P, Moulford, W B F L and Pearce, A J, "Erosion measurements for two- and three-grid ion thruster extraction systems", IEPC Paper 93-171, (September 1993).
- ⁹ Leiter, H, Feili, D., "RITAS a Radiofrequency Ion Engine for High Specific Impulse Operations", AIAA Paper 2001-3491.

¹⁰ Fearn, D G, “The application of gridded ion thrusters to high thrust, high specific impulse nuclear-electric missions”, IAF Paper IAC-04-R.4/S.7.09, (October 2004).

¹¹ Walker, R., Izzo, D., Fearn, D.G., “Missions To The Edge Of The Solar System Using A New Advanced Dual-Stage Gridded Ion Thruster With Very High Specific Impulse”, paper ISTS 2006-k-35, 25th International Symposium on Space Technology and Science, Kanazawa, Japan, 4-11 June 2006.

¹² Bramanti, C., Walker, R., Izzo, D., Fearn, D.G., Samaraee, T., “Very High Delta-V Missions to the Edge of the Solar System and Beyond Enabled by the Dual-Stage 4-Grid Ion Thruster Concept”, paper IAC-06-D.2.8.3 (October 2006)